

NISTIR 6030

**THIRTEENTH MEETING OF THE UJNR
PANEL ON FIRE RESEARCH AND SAFETY,
MARCH 13-20, 1996**

VOLUME 2

Kellie Ann Beall, Editor

June 1997
Building and Fire Research Laboratory
National Institute of Standards and Technology
Gaithersburg, MD 20899



U.S. Department of Commerce
William M. Daley, *Secretary*
Technology Administration
Gary R. Buchula, *Acting Under Secretary for Technology*
National Institute of Standards and Technology
Robert E. Hebner, *Acting Director*

EXPERIMENTS ON SMOKE BEHAVIOR IN CAVITY SPACES
Part 3 In case of the cavity space which has an opening at the bottom

Takeyoshi TANAKA
Building Research Institute, Ministry of Construction
1 Tatehara, Tsukuba-shi, Ibaraki-ken, 305 Japan

Teruhisa FUKUDA and Takao WAKAMATSU
Science University of Tokyo
2641 Yamasaki, Noda-shi, Chiba-ken, 278 Japan

ABSTRACT

It was demonstrated by the previous experiments using the cavity space which has no bottom opening that the temperature rise of plume at the height of the cavity opening is well scaled by the nondimensional temperature defined as $\Theta \equiv (\overline{\Delta T} / T_{\infty}) / \dot{Q}^{2/3}$ where $\dot{Q}^* \equiv \dot{Q} / \rho_{\infty} C_p T_{\infty} \sqrt{g D} D^2$, and the temperature is successfully correlated by $\Theta = \alpha (H/D)^b$, where $b = -5/3, -1$ and $-1/3$ for shallow, intermediate and deep cavity, respectively.

In this study, the smoke behavior in cavity spaces is further investigated by the small scale experiments for the cavity space which has an opening at the bottom. It was found that the larger the area of the bottom opening, the more stable the fire plume, but still the temperature is well correlated by the same manner as in the case of cavity with no bottom opening. Also, the effects of bottom opening on the temperature and the pressure difference produced in the cavity are analyzed.

KEYWORDS: smoke behavior, cavity space, fire plume, bottom opening, plume temperature, pressure difference, air inflow rate

1. INTRODUCTION

The primary issue of cavity spaces of buildings concerning fire safety is the potential hazard that such spaces may become a dominant passage of smoke spread throughout the buildings. Some means to predict the smoke behavior in cavity spaces will be necessary for rational measures for evacuation safety in the buildings having such cavity like spaces.

In the previous papers, the formulas for predicting the temperature elevation of the plumes as a function of heat release rate of fire and cavity dimensions were obtained for the cases where no opening exist at the bottom of the space. On the other hand, some cavity spaces in buildings have openings near the bottom. In Japan, building officials and fire department suspect that the air supply through such an opening contribute to mitigate the smoke hazard, so tend to insist on the equipment of opening for the cavity space exceeding certain depth. However, virtually no solid data is available for assessing how effective the openings are or how large they should be.

While all the air entrained to a fire plume is supplied through the opening at the top in case of the cavity having no bottom opening, the air will be supplied both from the top and the bottom in case of the cavity having bottom openings. The portion of the air supplied from the bottom may increase as the area of the bottom opening increases. Consequently, the existence of a bottom opening may significantly affect the smoke behavior in a cavity. In this study, reduced scale experiments are conducted for the cases where an opening exists at the bottom of a cavity, and the effects of the bottom opening size on the plume temperature and the pressure profile in the cavity are investigated.

2. EXPERIMENTAL SETUP

The cavity space model used in this experiment is the same as in the preceding experiments[1]: It has the square floor of 0.8m x 0.8m whose height can be changed from 0m to 3m using wires and a pulley. The tests are carried out for the depth of the cavity increased by every 0.25m from 0.25m to 3.0m.

A 7cm diameter diffusion burner is used as the fire source and the heat release rate is set at 0.5, 1.0, 2.0, 3.0 and 4.0kW according to the test conditions by adjusting the rate of supply of methane. The fire source in this experiment is set on the center of the floor, as shown in Figure 1.

The bottom opening in each test is arranged on the floor about uniformly around the fire source as shown in Figure 1 to maintain symmetric condition as best as possible and also to avoid the brown down of flames due to the draft induced through the opening. The area of the opening is 0.03, 0.067 or 0.163m² depending on the test conditions.

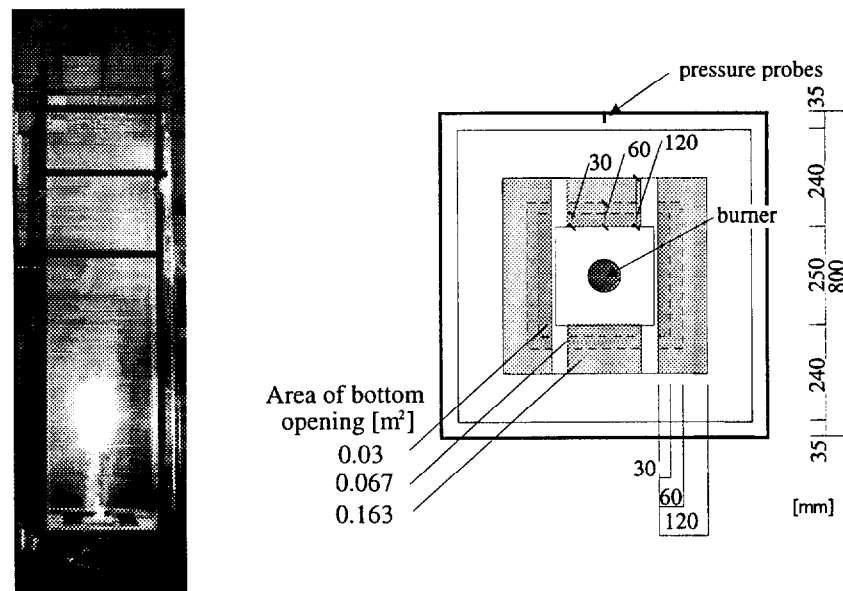


Figure 1 Arrangement of Bottom Opening

The measurements made are also the same as in Ref.[1]: 85 thermocouples are arrayed about uniformly over the opening at the top of the space to measure the temperatures of the gases flowing out of and the air flowing into the space; Pressure probes arranged at 10 positions on the rear wall for the measurement of the pressure difference between the inside of the cavity and the outside of the cavity space. The data acquisition is started 15 minutes after the ignition of the fire source and in each condition, the data recording is carried out for 5 minutes with 5 second interval.

3. RESULTS OF THE EXPERIMENTS

3.1 Temperature Profile at Top Opening

Figure 2 compares the typical temperature profiles at the opening at the top of the cavity for different area of the bottom opening. The heat release rate of the source for the examples in Figure 2 is 2.0kW and the cavity depth is 0.5m or 3.0m.

As can be seen from the figures for $H=0.5m$, the larger the bottom opening area, the steeper the temperature profile, when cavity depth is small. On the other hand, the larger the bottom opening area, the more dull the temperature profile tend to be, when cavity depth is large.

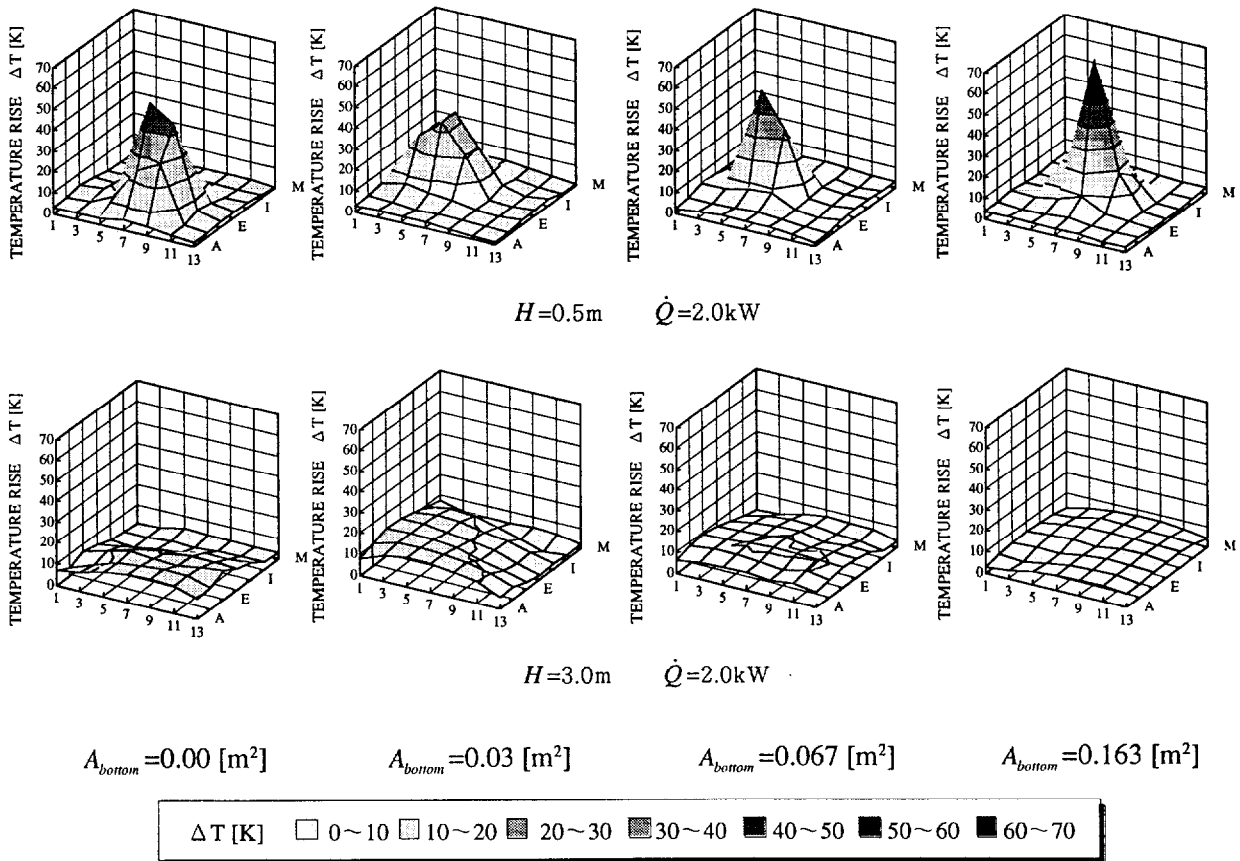


FIGURE 2 Temperature Profile at Top Opening

3.3 Fluctuation of Plume Axis

Figure 3 shows some examples of the frequency that each of the 85 thermocouples arrayed at the cavity opening recorded the highest temperature in the 60 times measurements, which were made during the 5 minutes of the data acquisition period. The examples are taken from the cases where the heat release rate is 2.0 kW and the cavity depth is 1.0m and 2.0m.

Here we assume that the plume axis exists around the position of the thermocouples at which the highest temperature is recorded. It can be seen from Figure 3 that the increase of the bottom opening area contributes to the stability of the location of the fire plume axis. This effect is particularly remarkable when the cavity depth is large, but still apparent when the cavity depth is small.

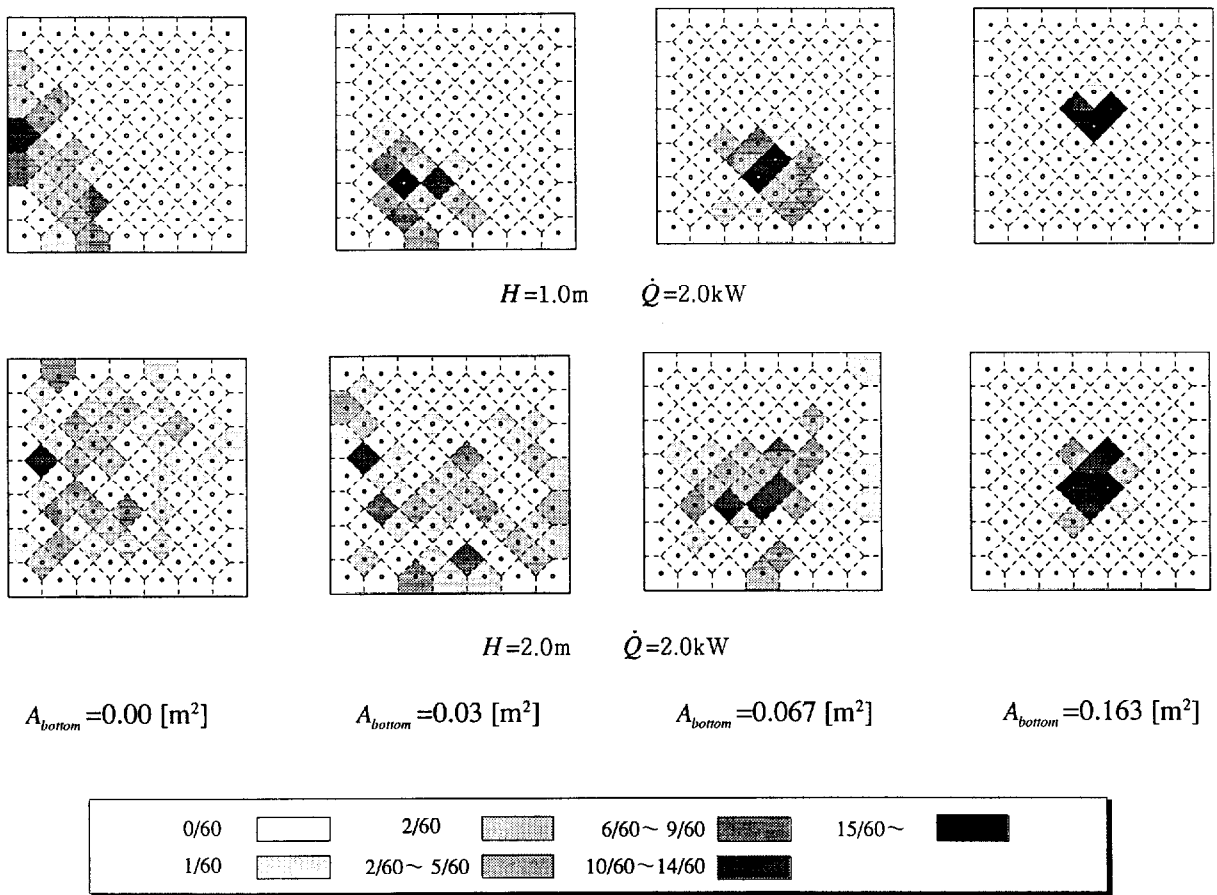


FIGURE 3 Fluctuation of Plume Axis

3.4 Vertical Profile of Pressure Difference

Figure 4 shows the profile of the pressure difference which develops between the inside and the outside of the 3.0m deep cavity space. Each value of the pressure difference is the average of the 60 times of data recordings in each test. The pressure difference of the cavity space relative to the outside space is nearly zero or slightly negative at the height of the cavity opening and increases about proportionally to the distance from the opening, but the increase seems to deter around the middle height of the cavity.

The pressure difference increases with the heat release rate when the area of the bottom opening is the same, and decreases as the bottom opening area increases if the heat release rate is the same.

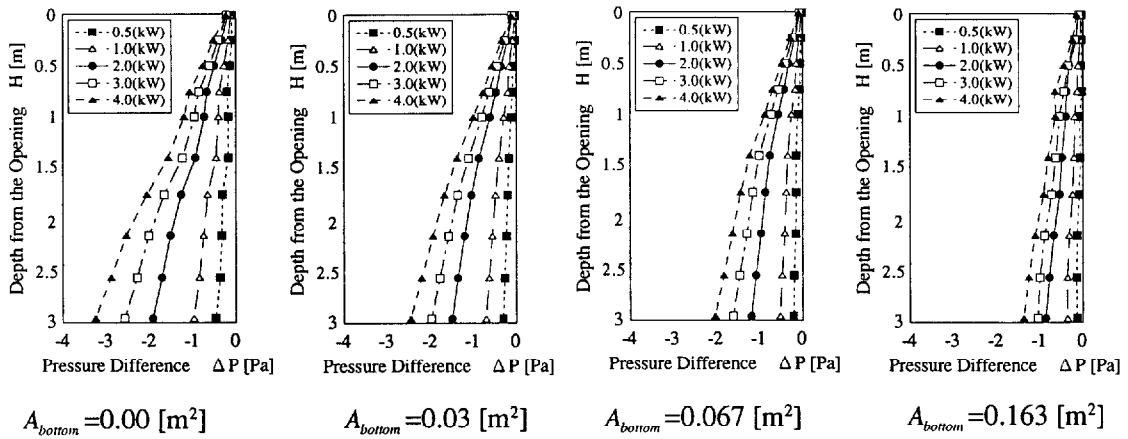


FIGURE 4 Pressure Difference

3.5 Plume Area

The proportion of the plume horizontal area at the height of the opening of the cavity to the floor area of the cavity (plume area ratio) is plotted versus the depth of the cavity in Figure 5. The plume area was assumed as the area in which the thermocouple readings fall in the condition as follows:

$$\Delta T \geq (T_{max} - T_{\infty}) \times k \quad (1)$$

with $k=0.25$, where T_{max} , T_{∞} and ΔT are the highest temperature reading of the thermocouples, the ambient air temperature and the temperature difference of a thermocouple from the ambient air.

Similarly with the findings previously reported for the cavity space having no bottom opening, the plume area does not depend on the heat release rate and tends to increase with the cavity depth H approximately in proportional to H^2 , H^1 and H^0 when the depth is small, intermediate and large, respectively. The plume area ratio for large cavity depth tends to increase with the increase of the bottom opening area, but the depth at which the transition from intermediate to deep region takes place seem to increase.

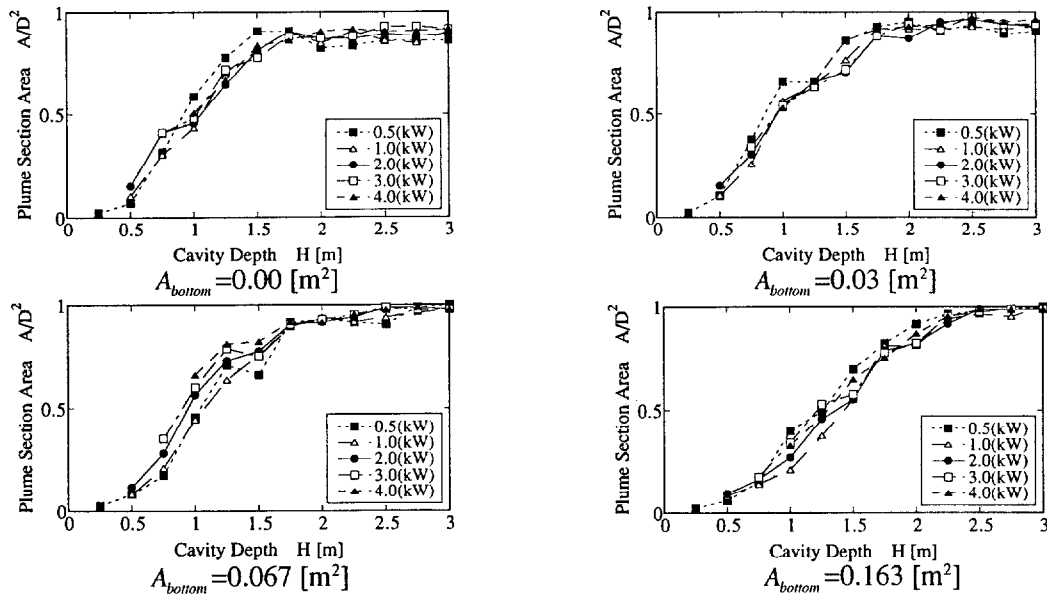


FIGURE 5 Plume Section Area A/D^2

3.6 Average Temperature Rise of the Fire Plume

The average temperature within the plume area defined by Eqn.(1) with $k=0.25$ is plotted versus the depth of the cavity in Figure 6. Each value of the temperatures in the figure is the average of the plume average temperatures for the 5 minutes of data acquisition period, each of which is obtained at every 5 seconds by averaging the temperatures within the plume area that is defined at each time according to Eqn.(4).

A similar tendency is observed in the temperature rise regardless the difference in bottom opening area as shown in Figure 7, i.e.: the temperatures fall significantly with the cavity depth while the depth is small, but it changes only slightly when the depth is large. The larger the bottom opening area, the lower the temperatures for large depth seem, if the heat release rate is the same.

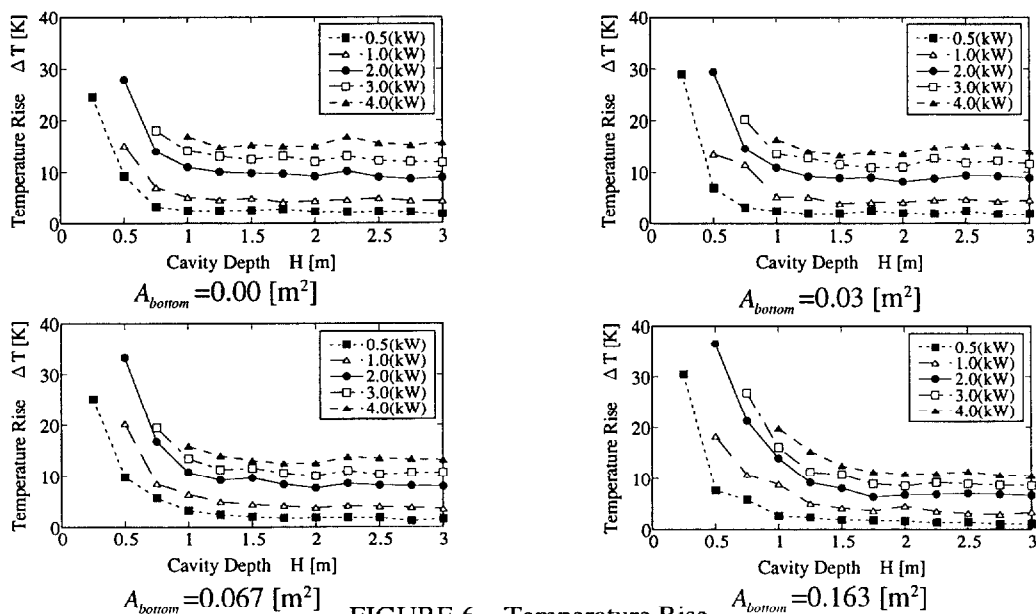


FIGURE 6 Temperature Rise

4. EQUATIONS FOR PLUME TEMPERATURE

In the preceding paper[1],[2], it was theoretically predicted and experimentally verified for the cavity having no bottom opening that the temperature of the fire plume in cavity spaces is well correlated as

$$\Theta = \alpha(H/D)^\beta \quad (2)$$

where β is $-5/3$, -1 and $-1/3$ for shallow, intermediate and deep cavity, respectively, Θ is the nondimensional temperature defined as

$$\Theta \equiv (\overline{\Delta T} / T_\infty) / \dot{Q}^{*2/3} \quad (3)$$

and \dot{Q}^* is the nondimensional heat release rate defined as

$$\dot{Q}^* \equiv \dot{Q} / \rho_\infty C_p T_\infty \sqrt{g D D^2} \quad (4)$$

Since it is considered that essentially the same theoretical consideration holds for the cavities with bottom openings, the equations for correlating the plume temperature are derived having the same relationship as Eqns.(2) -(4) in mind.

4.1 Equations for Plume Average Temperature

The plume average temperature here means the average of the temperatures within the area that is defined by Eqn.(1) with $k=0.25$. The temperatures are nondimensionalized in the form of Eqn.(2) and plotted versus H/D as shown in Figure 7. The solid and the broken lines in the figures indicate the regression lines when the theoretical and the experimental values are employed for β in Eqn.(2), respectively. The values α and β of the theoretical and experimental regression equations are summarized in Table 1. Note, however, that α cannot be theoretically obtained in either case. The values of α in the column of "theoretical value" are in reality the experimental values that fit well with the test data provided the theoretical β is used. Since it does not make meaningful difference in the accuracy whichever of the values may be used for β , as is recognized from the insignificant difference between the solid and broken lines, the equations adopting the theoretical β may be sufficiently adequate for plume average temperature.

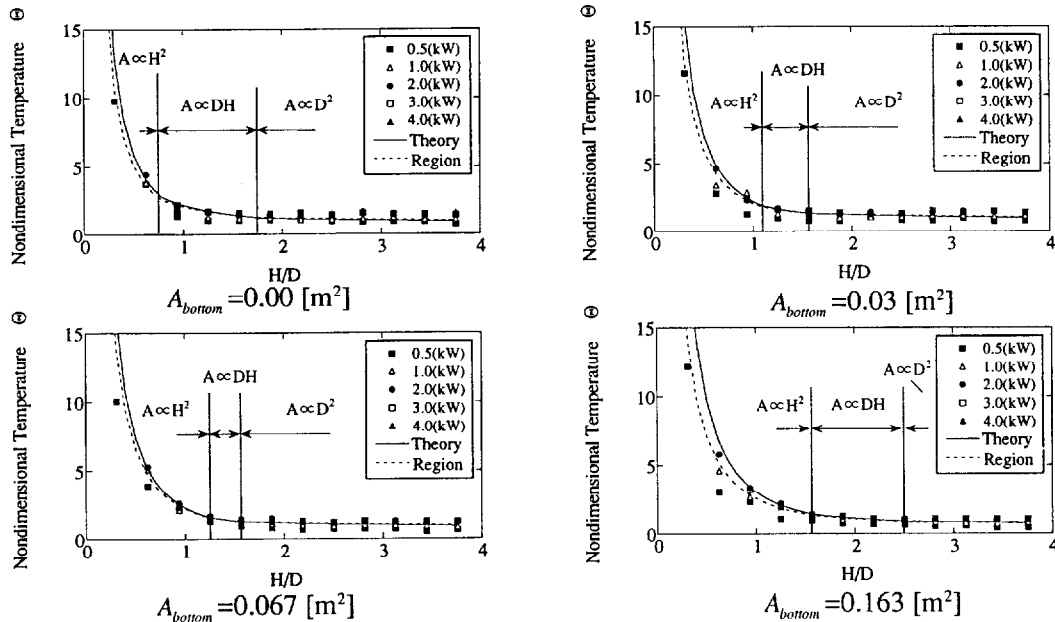


FIGURE 7 Nondimensional Temperature

Table 1 Comparison with the values α and β of the theoretical and experimental regression

Opening Area [m ²]	Region	Experiments		Theory	
		α	β	α^{*1}	β
0.00	$H/D \leq 0.78$	1.74	-1.55	1.86	-5/3
	$0.78 < H/D \leq 1.77$	2.09	-0.90	2.19	-1
	$1.77 < H/D$	1.48	-0.28	1.48	-1/3
0.03	$H/D \leq 1.09$	2.07	-1.53	2.23	-5/3
	$1.09 < H/D \leq 1.56$	1.93	-0.81	2.09	-1
	$1.56 < H/D$	1.51	-0.26	1.56	-1/3
0.0672	$H/D \leq 1.25$	2.23	-1.56	2.33	-5/3
	$1.25 < H/D \leq 1.56$	1.91	-0.86	2.01	-1
	$1.56 < H/D$	1.45	-0.26	1.49	-1/3
0.1632	$H/D \leq 1.56$	2.60	-1.45	3.08	-5/3
	$1.56 < H/D \leq 2.50$	2.07	-0.93	2.29	-1
	$2.50 < H/D$	1.16	-0.30	1.24	-1/3

4.2 Dependence of Plume Temperature for Large Depth on Bottom Opening Area

It is considered that the smoke hazard in cavity spaces is particularly serious for deep cavity: When H/D is small the contamination by smoke will be confined to a limited part of the space just like by window jets ejecting to outdoor. But when H/D is large the space can be extensively subjected to the influence of smoke.

As can be recognized from the values of coefficient α for large H/D in Table 1, the temperatures for large depth decrease with the increase of the bottom opening area, so providing bottom opening may help mitigate the smoke hazard. Here we introduce the bottom opening ratio γ : the ratio of bottom opening area to horizontal section area of cavity, namely

$$\gamma \equiv A_{\text{bottom}} / D^2 \quad (5)$$

The reason why the temperature for large depth decrease with the increase of the bottom opening area is suspected to be because the rate of the air supply through the opening at the top of the cavity space decreases as the bottom opening area increases, so more fresh air is entrained into the fire plume. Nevertheless, the air supplied from the top of the cavity has a significant effect on diluting the fire plume gases even when A_{bottom} is zero. Since it is considered that both of the air supply from the top and the bottom have significant effect on the temperatures, the values of coefficient α for large H/D are plotted in Figure 8 versus

$$\frac{A_{\text{bottom}} + D^2}{D^2} = \gamma + 1 \quad (6)$$

instead of simply plotting versus γ . Note that the value of for $\gamma=0$ (no bottom opening) is taken from the previous paper. The experimental correlation between α and γ can be established as

$$\Theta = 1.67(\gamma + 1)^{-4/3} \quad (7)$$

Note, however, that the discrepancy of the value of for $\gamma=0$ from the regression line was disregarded.

Substituting Eqns.(7) into Eqn.(2) yields the generalized formula for the plume temperature for large H/D as follows:

$$\Theta = 1.67(\gamma + 1)^{-4/3} (H/D)^{-1/3} \quad (8)$$

The application of Eqn.(8) should be conservatively confined within $0 < \gamma < 0.25$, since the applicability beyond this region has not been confirmed either experimentally nor theoretically. However,

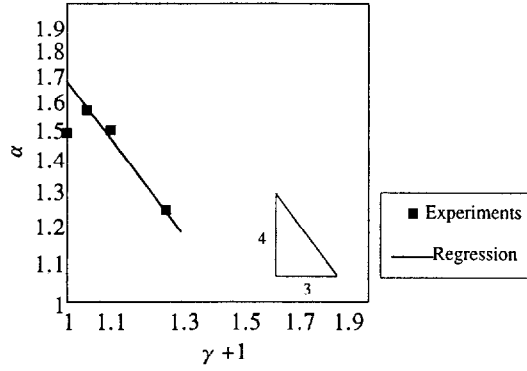


FIGURE 8 Bottom opening ratio and α

considering the bottom opening area ratio of the existing cavity spaces, the application of Eqn.(8) will not be so limited.

5. PRESSURE DIFFERENCE

5.1 Nondimensional Pressure Difference

The pressure difference which develops between the inside and the outside of a cavity space affects the measures for protecting the floor area adjacent to the cavity space from the infiltration of smoke. According to Figure 4, which shows the pressure difference profile for the cavity with 3m depth, the pressure difference is nearly zero at the height of the top opening regardless the difference in the heat release rate and the bottom opening area, but differs depending on the conditions.

Although the exact mechanism of the pressure development is not obvious, since the pressure difference increases with the distance from the top, at least down to the middle height, the pressure difference at the bottom ΔP_{bottom} may be assumed as

$$\Delta P_{bottom} \propto \Delta \rho g H \quad (9)$$

Dividing the both side of Eqn.(9) by $\Delta \rho_{\infty} g H$ and noting that for large H/D the relationship as

$$\frac{\Delta T}{T_{\infty}} \propto \dot{Q}^{2/3} \left(\frac{H}{D} \right)^{-1/3}$$

has been obtained, we have

$$\frac{\Delta P_{bottom}}{\rho_{\infty} g H} \propto \frac{\Delta \rho}{\rho_{\infty}} \approx \frac{\Delta T}{T_{\infty}} \propto \dot{Q}^{2/3} \left(\frac{H}{D} \right)$$

However, this presumption may fail because the temperature of the lower part of a cavity space cannot be represented by the plume temperature. Hence, based on the above consideration, we introduce the nondimensional pressure π defined as

$$\pi \equiv (\Delta P_{bottom} / \rho_{\infty} g H) / \dot{Q}^{2/3} \quad (10)$$

and investigate the dependence of π on cavity depth.

In Figure 9, the nondimensional pressure π for cavity with different depth are plotted versus H/D of cavity. According to Figure 9, the data for 2.0, 3.0 and 4.0kW fire are collapse to a single line in each bottom opening size, which implies that the pressure difference is well scaled by π . Although the data for 0.5 and 2.0kW fire are not necessarily in good agreement, this is thought to be because the fire sizes are too small to induce the pressure large enough for the accurate measurement.

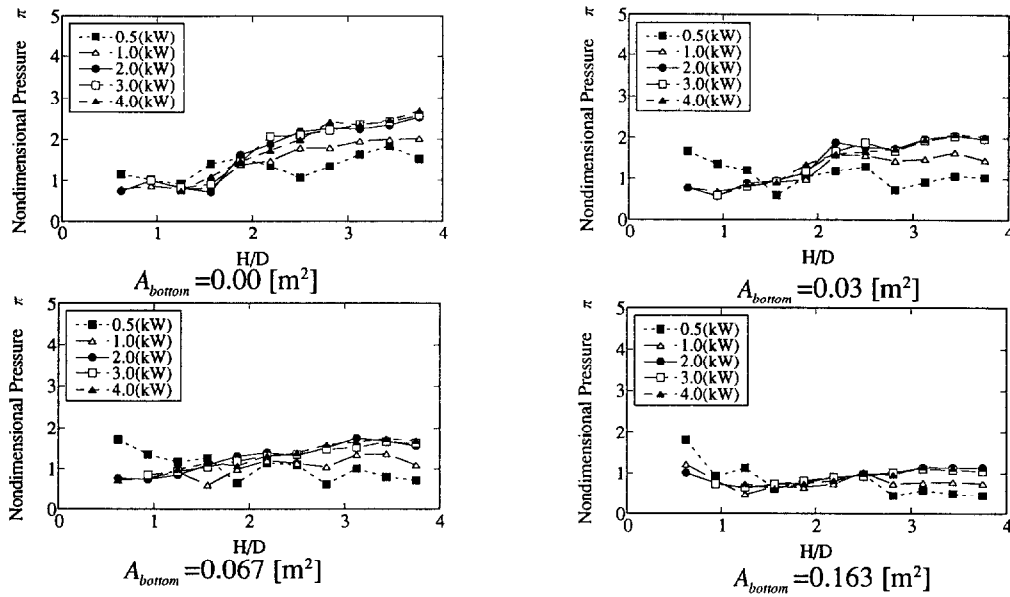


FIGURE 9 Nondimensional Pressure

5.2 Dependence of Pressure Difference on Bottom Opening Area

Looking at Figure 9, π is about constant where H/D is large and proportional to H/D where H/D is intermediate, while a consistent tendency cannot always be observed where H/D is small. In order to investigate the dependence of the pressure difference on bottom opening area, π for cavity space with large H/D and 2.0, 3.0 and 4.0kW fire is plotted versus $\gamma+1$ in Figure 10. The regression line can be expressed as

$$\pi = 2.3(\gamma+1)^{-10/3} \quad (11)$$

Since the boundary of intermediate and large depth seem to be somewhere around $H/D=2.5$, let's regard Eqn.(11) apply for $H/D>2.5$. Then, where cavity depth is intermediate, noting that π increases about proportionally to H/D , π may be given as

$$\pi = 0.92(\gamma+1)^{-10/3}(H/D) \quad (12)$$

From Figure 11, which compares the experimental data and Eqns.(11) and (12), Eqn.(12) is considered to be applicable roughly for $1.2 < H/D < 2.5$.

Incidentally, Eqns.(11) and (12) should be considered to be applicable for $0 < \gamma < 0.25$ with respect to the bottom opening area.

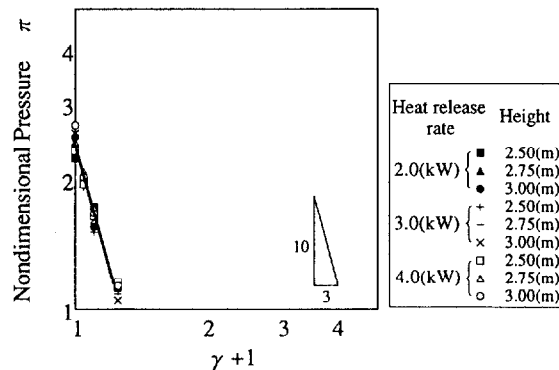


FIGURE 10 Bottom opening ratio and Nondimensional Pressure

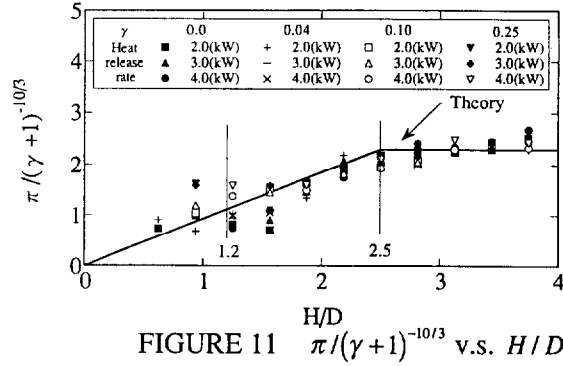


FIGURE 11 $\pi/(\gamma+1)^{-10/3}$ v.s. H/D

6. RATE OF AIR INFLOW THROUGH BOTTOM OPENING

The rate of air inflow through the bottom opening m_{bottom} is given by

$$m_{bottom} = C_D A_{bottom} \sqrt{2\rho_\infty \Delta P_{bottom}} \quad (13)$$

Substituting Eqn.(10) into Eqn.(13), we have

$$m_{bottom} = C_D \rho_\infty A_{bottom} \sqrt{2gH\pi \dot{Q}^{*1/3}} \quad (14)$$

Introducing the nondimensional flow rate defined as

$$\mu \equiv (m_{bottom} / \rho_\infty \sqrt{gD^5}) / \dot{Q}^{*1/3} \quad (15)$$

and substituting this into Eqn.(14) yields

$$\mu = C_D \sqrt{2} (A_{bottom} / D^2) \pi^{1/2} (H/D)^{1/2} = C_D \sqrt{2} \gamma \pi^{1/2} (H/D)^{1/2} \quad (16)$$

Using Eqns.(11) and (12), and letting $C_D=0.7$, we have

$$\mu = \begin{cases} 0.95 \frac{\gamma}{(\gamma+1)^{5/3}} \left(\frac{H}{D}\right) & (1.2 < H/D < 2.5) \\ 1.50 \frac{\gamma}{(\gamma+1)^{5/3}} \left(\frac{H}{D}\right)^{1/2} & (2.5 \leq H/D) \end{cases} \quad (17)$$

Figure 12 shows the comparison of Eqn.(17) and the nondimensional air inflow rate from the measurement. Notice that the latter is calculated by using the pressure difference measured at the bottom to Eqn.(17), hence the comparison of air inflow rates in Figure 12 is nothing but a different form of the comparison of the pressure difference in Figure 11.

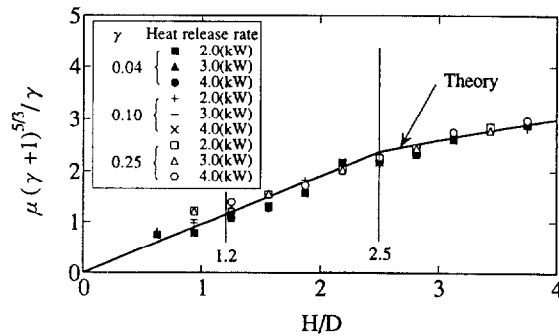


FIGURE 12 $\mu(\gamma+1)^{5/3}/\gamma$ v.s. H/D

7. CONCLUDING REMARKS

The experiments were conducted for elucidating the behavior of fire plume in the cavity which has an opening at the bottom. It was found that the larger the bottom opening, the more stable the fire

plume, but still the temperature is correlated by the same manner as in the case of cavity with no opening.

The effects of the bottom opening area on the plume temperature, the pressure difference induced in the cavity space and the mass inflow rate of air through the bottom opening are investigated and the experimental correlations were obtained.

NOMENCLATURE

A	Horizontal section area of fire plume (m ²)
A_{bottom}	Area of bottom opening (m ²)
C_p	Specific heat of air (kJ/kgK)
C_D	Flow Coefficient
D	Length of the side of cavity space (m)
g	Acceleration due to gravity (m/s ²)
H	Depth of cavity (m)
m_{bottom}	Rate of air inflow through bottom opening(kg/s)
γ	Bottom opening ratio
ΔP	Pressure difference (Pa)
ΔP_{bottom}	Pressure difference at the bottom of cavity space (Pa)
\dot{Q}	Heat release rate of fire source (kW)
\dot{Q}^*	Nondimensional heat release rate
T	Temperature (K)
T_∞	Ambient temperature (K)
ΔT	Temperature difference (K)
α	Coefficient of Eqn.(2)
β	Factor of Eqn.(2)
ρ_∞	Ambient air density
π	Nondimensional pressure
μ	Nondimensional flow rate
Θ	Nondimensional temperature

REFERENCES

- [1] Takeyoshi TANAKA and Sunao KUMAI : Experiments on Smoke Behavior in Cavity Spaces,
- [2] Takeyoshi TANAKA, Sunao KUMAI, Teruhisa FUKUDA, Akihiko YOSHIKAWA, Osamu ISHINO, and Takao WAKAMATSU: Smoke Behavior in Cavity Spaces, Part 1 In case where the fire sources are located at the center of the cavity floor,
- [3] Teruhisa FUKUDA, Akihiko YOSHIKAWA, Sunao KUMAI, Osamu ISHINO, Takeyoshi TANAKA and Takao WAKAMATSU: Smoke Behavior in Cavity Spaces, Part 2 In case where the fire sources are located by a wall or at a corner,

Discussion

Edward Zukoski: Is the wind direction important in the original problem, whether the opening to the lower air cavity is upwind or downwind?

Takeyoshi Tanaka: I haven't looked at that problem yet. Whether or not wind is important will be determined by the relationship between the size of heat release and the height of the cavity.

Tokiyoshi Yamada: There is some pressure difference and I think the pressure difference was zero at the top. When at lower part is closed, I believe that vertical flow occurs but could you tell us where the flood occurred.

Takeyoshi Tanaka: I do not know.